



Pyrazolopyridines as a novel structural class of potent and selective PDE4 inhibitors

J. Nicole Hamblin^{*}, Tony D. R. Angell, Stuart P. Ballantine, Caroline M. Cook, Anthony W. J. Cooper, John Dawson, Christopher J. Delves, Paul S. Jones, Mika Lindvall[†], Fiona S. Lucas, Charlotte J. Mitchell, Margarete Y. Neu, Lisa E. Ranshaw, Yemisi E. Solanke, Don O. Somers, Joanne O. Wiseman

GlaxoSmithKline Medicines Research Centre, Gunnels Wood Road, Stevenage, Hertfordshire SG1 2NY, UK

ARTICLE INFO

Article history:

Received 8 April 2008

Revised 13 May 2008

Accepted 14 May 2008

Available online 17 May 2008

Keywords:

PDE4 inhibitors

SAR

Crystallography

Pyrazolopyridine

ABSTRACT

Optimisation of a high-throughput screening hit resulted in the discovery of 4-(substituted amino)-1-alkyl-pyrazolo[3,4-*b*]pyridine-5-carboxamides as potent and selective inhibitors of Phosphodiesterase 4 (PDE4). Herein, we describe early SAR studies around this novel template highlighting preferred substituents and rationalization of SAR through X-ray crystal structures of analogues bound to the PDE4 active site. Pyrazolopyridine **20a** was found to be a potent and selective PDE4 inhibitor which also inhibits LPS induced TNF- α production from isolated human peripheral blood mononuclear cells and has an encouraging rat PK profile suitable for oral dosing.

© 2008 Elsevier Ltd. All rights reserved.

Chronic obstructive pulmonary disease (COPD)¹ is a leading cause of morbidity and mortality worldwide, forecast to become the fifth leading cause of death by 2020. Cigarette smoking is the principal risk factor and the disease is characterised by progressive, largely irreversible airflow obstruction, significant structural damage and by the presence of one or more of the following pathologies: chronic bronchitis, emphysema and bronchiolitis. Phosphodiesterase 4 (PDE4) plays a key role in the regulation of intracellular concentrations of the second messenger cyclic AMP (cAMP), effecting its selective hydrolysis to 5'-AMP. PDE4 is the predominant phosphodiesterase enzyme in immune and inflammatory cells (e.g. neutrophils, monocytes, macrophages)² and is also a major contributor to cAMP metabolism in airway smooth muscle and airway epithelial cells.³ In COPD, cAMP is believed to suppress the activation of immunocompetent cells, mediate bronchodilation, modulate neuronal activity and inhibit smooth muscle proliferation; hence elevated levels of cAMP achieved through PDE4 inhibition may be beneficial for COPD patients.⁴

PDE4 inhibitors are known to have a broad range of anti-inflammatory and anti-bronchoconstrictor effects in animal models⁵ and as such have been well studied by numerous groups.⁶ In spite of this however, bringing a drug of this class to market has been hampered by undesirable side effects. Early PDE4 inhibitors such as

Rolipram **1** cause pronounced nausea and emesis at effective anti-inflammatory doses in the clinic.⁷ Roflumilast (Daxas[™]) **2** is representative of a second generation of PDE4 inhibitors which show moderate efficacy in COPD at tolerated doses,⁸ however, the maximum dose that can be given (and hence efficacy) is still limited by the aforementioned transient adverse effects.

Our objective was thus to develop an oral PDE4 inhibitor with improved therapeutic index.

At the time we began our work, most of the advanced PDE4 inhibitors possessed a common catechol ether structural motif (Fig. 1). Our initial strategy was to determine whether this was contributing to the observed emetic effects and hence we sought a lead molecule devoid of this structural feature. Compound **3** (Fig. 2) was discovered via high throughput screening, along with several structurally related pyrazolopyridine analogues which all showed good PDE4 potency and promising selectivity profiles versus PDE3 and PDE5.⁹ There are four sub-types of the PDE4 enzyme: A, B, C and D, but the PDE4B sub-type is believed to play a central

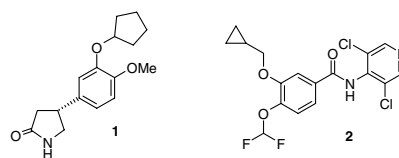


Figure 1. Structures of *R*-Rolipram **1** and Roflumilast **2**.

^{*} Corresponding author. Fax: +44 (0)1438 768301.

E-mail address: nicole.j.hamblin@gsk.com (J.N. Hamblin).

[†] Present address: Novartis Institute for Biomedical Research, 4560 Horton Street, Emeryville, CA 94607, USA.

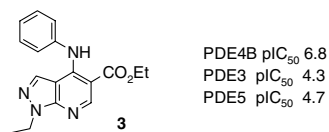


Figure 2. Initial pyrazolopyridine HTS hit.

role in inflammation,¹⁰ being the predominant subtype in monocytes and neutrophils and hence we used this isoform for routine screening.

The series was considered highly tractable and sufficiently structurally distinct from known PDE4 inhibitors to be an interesting start point. Initial plans were to explore the SAR around the three existing substituents using parallel synthesis techniques.

Synthesis of pyrazolopyridines is well described in the literature and we chose to use the precedented high temperature reaction between *N*-1-ethyl-5-aminopyrazole **4** and diethyl ethoxymethylenemalonate **5** to form the ring (Scheme 1).^{11,12} 4-Hydroxypyrazolopyridine intermediate **6** was treated directly with phosphoryl chloride to give key 4-chloro-derivative **7**, which underwent thermal displacement with a diverse range of amines to give **8a–j**, allowing us to probe SAR at the 4-position.

The data showed that a significant increase in potency is observed where the 4-substituent is a branched or cycloalkyl amino-group, with 6-membered saturated rings more potent than 5-membered rings (Table 1). Particularly interesting was tetrahydropyran analogue **8e** with the data suggesting that polar functionality can be tolerated and that this position may therefore offer a handle for future modification of physicochemical properties, should this be required during lead optimisation.

Tertiary amines such as pyrrolidine in **8c** were less preferred, as were *N*-methylated analogues such as **8j** suggesting the importance of the NH group. These observations were later explained by crystal structures of related pyrazolopyridine analogues bound to PDE4B (Fig. 3), which showed the presence of an internal hydrogen bond between the 4-NH group and the 5-carbonyl oxygen, to maintain planarity with the template. Unbranched alkyl amines gave poor selectivity over PDE5, in contrast to branched analogues which routinely gave >100-fold selectivity (data not shown).

We also chose to investigate the nature of the linking group at the 4-position (Scheme 1). Displacement of chlorine in intermediate **7** with azide and reduction under Staudinger conditions¹³ afforded 4-amino intermediate **10**, which was derivatised under standard conditions to provide amide and sulphonamide derivatives. Unfortunately these changes afforded a general loss of potency (Table 1), again supported by the crystal structure which showed that the conformational restriction required to allow the

Table 1

Pyrazolopyridine 4-position SAR

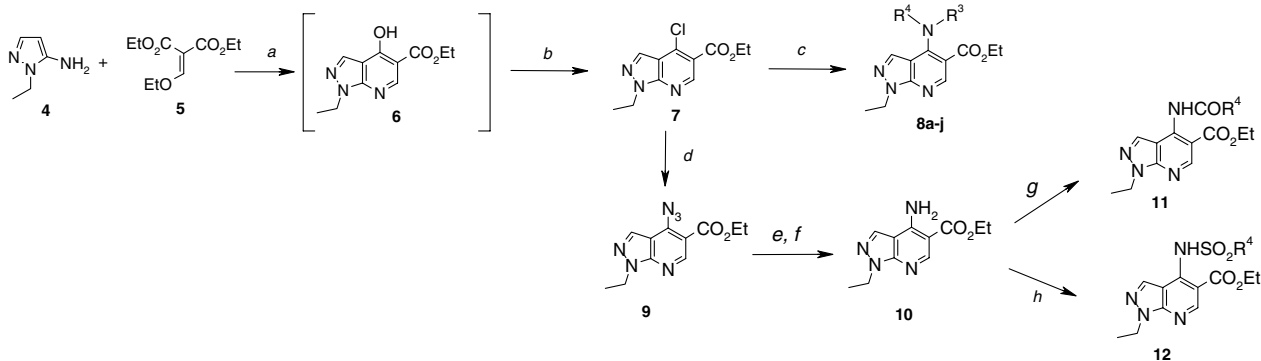
| | R ⁴ | PDE4BpIC ₅₀ ^a |
|------------|----------------------|-------------------------------------|
| 8a | | 6.8 |
| 8b | | 7.2 |
| 8c | | 6.2 |
| 8d | | 8.0 |
| 8e | | 7.8 |
| 8f | | 7.8 |
| 8g | | 6.7 |
| 8h | | 6.0 |
| 8i | | 6.5 |
| 8j | | 6.6 ^b |
| 11a | NHCOPh | 5.6 |
| 12a | NHSO ₂ Ph | <4.5 |

^a Values are mean of ≥2 experiments in all tables unless otherwise stated.

^b Value is a single experiment.

aforementioned intramolecular hydrogen bond was unfavourable with these alternative linkers.

Chemistry to introduce variation at the 1-position followed the published method of Bare et al.¹¹ (Scheme 2). Preparation of the versatile 1-H pyrazolopyridine intermediate **13** from compound **7** first required transformation of the 4-chloro substituent into the



Scheme 1. Reagents and conditions: (a) 150 °C, neat, 16 h; (b) POCl₃, 120 °C, 20 h (58% over two steps); (c) R⁴R³NH, EtOH, Et₃N, 80 °C, 16 h; (d) NaN₃, DMF, 16 h (84%); (e) PPh₃, THF, 2.5 h; (f) H₂O 2 h (60% over two steps); (g) R⁴COCl, CHCl₃, Et₃N, 16 h; (h) R⁴SO₂Cl, CHCl₃, pyridine, reflux, 72 h.

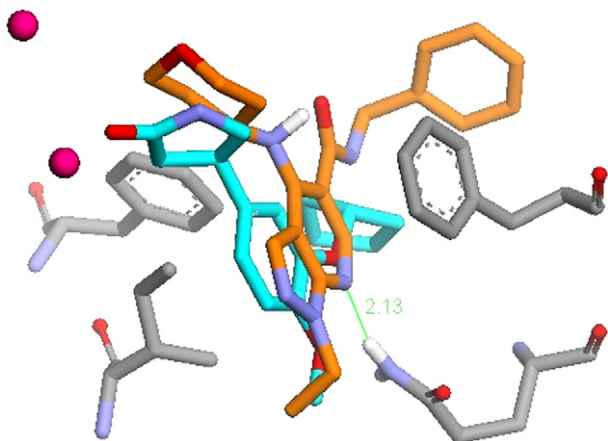
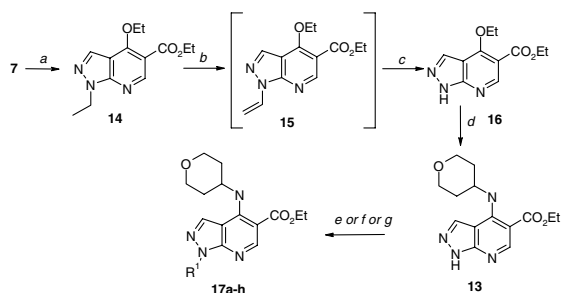


Figure 3. Overlay of the crystal structure of compound **20a** (orange) and *R*-Rolipram **1** (cyan) bound to PDE4B 152–503. Key amino acids are shown in grey and metal ions within the active site are shown in magenta.



Scheme 2. Reagents and conditions: (a) Na, EtOH, reflux, 2 h, 90%; (b) NBS, CCl₄, reflux, 3 h; (c) Na₂CO₃, THF, 18 h, 51% over two steps; (d) 4-aminotetrahydropyran, neat, 90 °C, 6 h, 91%; (e) *p*-BEMP resin, R¹Br, DMF, 16 h; (f) NaH, DMF, R¹Br, 16 h; (g) K₂CO₃, DMF, R¹Br, 55 °C, 45 h.

less reactive 4-ethoxy group in **14**, in order to avoid undesirable hydrolysis during subsequent steps. Bromination of the 1-ethyl group and in situ elimination then afforded vinyl derivative **15** which was used directly in the next step. N-dealkylation under basic conditions to give **16** was followed by incorporation of the preferred 4-amino tetrahydropyran moiety, to afford **13** which could be used to probe the 1-position SAR via alkylation.

A variety of different bases were used to deprotonate the pyrazolopyridine template in **13**, including sodium hydride, potassium carbonate and the polymer bound base BEMP (2-*tert* butylimino-2-diethylamino-1,3-dimethyl-perhydro-1,3,2-diazaphosphorine). The latter showed the greatest utility for our needs, allowing facile work up of multiple parallel reactions. The resultant anion was then treated with a range of alkyl halides.

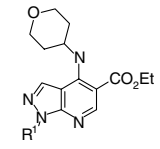
Compound **18** where R¹ = phenyl was prepared according to Scheme 1 starting with *N*-1-phenyl-5-aminopyrazole.

Unfortunately, this work failed to uncover a superior substituent to ethyl with respect to potency, the trend for simple alkyls and aryls following Et > Me, Pr, *i*-Pr > H, CH₂Ph, Ph (Table 2). Incorporation of more highly functionalised groups, such as the hydroxyethyl derivative **17h**, was generally detrimental for potency.

X-ray crystallography of related molecules bound to PDE4B (Fig. 3) later highlighted that the 1-ethyl substituent optimally fills a small pocket, the size constraint of which supports the observed SAR.

Since we were concerned about the potential for metabolic instability of the ester functionality and we desired orally bioavail-

Table 2
Pyrazolopyridine 1-position SAR



| | R ¹ | PDE4B pIC ₅₀ |
|------------|--|-------------------------|
| 17a | H | 5.7 |
| 17b | Me | 6.6 |
| 17c | Et | 8.0 |
| 17d | Pr | 7.0 |
| 17e | <i>i</i> -Pr | 6.7 ^b |
| 17f | CH ₂ Ph | 5.4 |
| 17g | (CH ₂) ₂ CO ₂ Et | 5.3 |
| 17h | (CH ₂) ₂ OH | 6.8 |
| 18 | Ph | 5.5 |

^b Value is a single experiment.

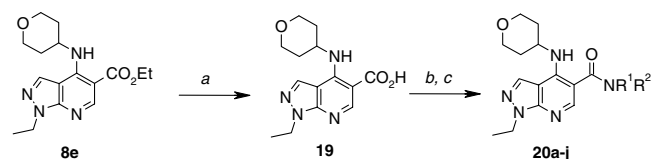
able inhibitors, we also prepared an array of 5-amides. For this work we elected to use our preferred tetrahydropyran amino substituent at the 4-position. Ester hydrolysis of **8e** was carried out using sodium hydroxide in aqueous ethanol and was followed by amide formation via the acid chloride under standard conditions.¹¹ The acid chloride was not isolated but was treated directly with a range of amines in a parallel fashion (Scheme 3).

The data showed the 5-position to be tolerant of a wide range of amide substituents (Table 3), again consistent with the crystal structure wherein this position is directed towards the opening of the active site (Fig. 3). In general, lipophilic secondary amides were well tolerated, with benzyl amides such as **20a** and saturated analogues such as **20j** preferred. Primary amide **20e** was acceptable but tertiary amides such as **20b** and cyclic amines such as **20f** afforded reduced potency.

Several amides of interest were selected for progression to further assays (Table 3). The data show that good cellular potency (inhibition of TNF-α in PBMCs¹⁴) can be achieved across this series. >100-fold selectivity versus PDE3 and PDE5 is also demonstrated.

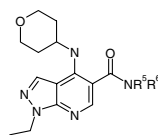
Examination of oral rat PK profiles for selected pairs of analogues showed, not surprisingly, that the 5-amide derivatives routinely gave improved bioavailability as compared with the 5-ester analogues. Compound **20a** was shown to have particularly encouraging rat oral PK [rat *t*_{1/2} 1.6 h, F 35%].

As referred to above, the crystal structure of compound **20a** bound to PDE4B 152–503¹⁵ (Fig. 3) shows the tetrahydropyran moiety directed towards the metal ions in the active site. An intramolecular hydrogen bond, between the 4-amino NH group and the carbonyl of the amide, maintains co-planarity with the template and orients the 5-benzylamine group towards the opening of the active site. The template itself sits in a 'hydrophobic clamp' formed by Ile410, Phe414 and Phe446. The pyridine-like nitrogen forms a hydrogen bond with Gln443 and the *N*-ethyl substituent fills the same small lipophilic pocket as occupied by the methoxy group of Rolipram.



Scheme 3. Reagents and conditions: (a) NaOH, EtOH/H₂O (95:5), 16 h, 97%; (b) SOCl₂, CHCl₃, 1 h; (c) R¹R²NH, 0 °C, 0.5 h.

Table 3
Pyrazolopyridine 5-position SAR



| | NR ⁵ R ⁶ | PDE4B pIC ₅₀ | PDE3 pIC ₅₀ | PDE5 pIC ₅₀ | PBMC TNF-α pIC ₅₀ |
|------------|--------------------------------|-------------------------|------------------------|------------------------|------------------------------|
| 20a | | 8.5 | <4.5 | 5.7 | 7.7 |
| 20b | | 7.3 | — | — | — |
| 20c | | 7.7 | <4.5 | 4.8 | 7.1 |
| 20d | | 7.9 | <4.5 | <4.7 | 7.4 |
| 20e | NH ₂ | 7.6 | <4.5 | 4.8 | 7.1 |
| 20f | | 6.8 | — | — | — |
| 20g | | 7.3 | <4.5 | <4.7 | 6.8 |
| 20h | | 6.9 | — | — | — |
| 20i | | 7.0 | — | — | — |
| 20j | | 8.1 | <4.5 | 5.5 | 7.2 |

In summary, a new series of 4-(substituted amino)-1-alkyl-pyrazolo[3,4-*b*]pyridine-5-carboxamides has been identified as potent and selective inhibitors of PDE4. The early SAR has been rationalized by crystallography and representatives from the series show good cellular potency, selectivity versus PDE3 and PDE5 and rat PK suitable for oral dosing. In particular, **20a** has emerged as a compound of significant interest.

Progress with in vivo studies towards the ultimate goal of providing a potent PDE4 inhibitor with a good therapeutic index from this series will be reported in due course.

Acknowledgements

The authors thank Giancarlo Trani for synthetic contributions whilst on placement at GSK.

References and notes

- Krishna, G.; Sankaranarayanan, V.; Chitkara, R. K. *Exp. Opin. Invest. Drugs* **2004**, *13*, 255, and references therein.
- Torphy, T. J.; Undem, B. J. *Thorax* **1991**, *46*, 512.
- Torphy, T. J.; Undem, B. J.; Cieslinski, L. B.; Luttmann, M. A.; Reeves, M. L.; Hay, D. W. P. *J. Pharmacol. Exp. Ther.* **1993**, *265*, 1213.
- Wang, D.; Cui, X. *Int. J. COPD* **2006**, *1*, 373.
- Bundschuh, D. S.; Eltze, M.; Barsig, J.; Wollin, L.; Hatzelmann, A.; Beume, R. J. *Pharmacol. Exp. Ther.* **2001**, *297*, 280.
- For recent reviews see McKenna, J. M.; Muller, G. W. In *Cyclic Nucleotide Phosphodiesterases in Health and Disease*, CRC Press LLC: Boca Raton, Florida, USA, 2007; p 667; Dyke, Hazel J. *Exp. Opin. Ther. Patents* **2007**, *17*, 1183; Smith, V. B.; Spina, D. *Curr. Opin. Invest. Drugs* **2005**, *6*, 1136.
- Horowski, R.; Sastre-Y-Hernandez, M. *Curr. Ther. Res.* **1998**, *38*, 23.
- Rabe, F.; O'Donnell, D.; Muir, F., et al. *Eur. Respir. J.* **2004**, *24*(Suppl. 48). Abst. 267.
- The ability of compounds to inhibit catalytic activity at PDE4B (human recombinant), PDE3 (from bovine aorta) and PDE5 (human recombinant) was determined by scintillation proximity assay (SPA) in 96-well format as described in WO2004024728.
- Wang, P.; Ohleth, K. M.; Wu, P.; Billah, M. M.; Egan, R. W. *Mol. Pharmacol.* **1999**, *56*, 170.
- Bare, T. M.; McLaren, C. D.; Campbell, J. B.; Firor, J. W.; Resch, J. F.; Walters, C. P.; Salama, A. I.; Meiners, B. A.; Patel, J. B. *J. Med. Chem.* **1989**, *32*, 2561.
- Yu, G.; Mason, H. J.; Ximao, W.; Wang, J.; Chong, S.; Dorrough, G.; Henwood, A.; Pongrac, R.; Seliger, L.; He, B.; Adam, L.; Krupinski, J.; Macor, J. J. *J. Med. Chem.* **2001**, *44*, 1025.
- Vaultier, M.; Knouzi, N.; Carrié, R. *Tetrahedron Lett.* **1983**, *24*, 763.
- PBMCs were prepared from heparinised human blood by centrifugation on hystopaque at 1000g for 30 min. The cells were collected from the interface, washed by centrifugation (1300g, 10 min) and resuspended in assay buffer (RPMI1640 containing 10% foetal calf serum, 1% L-glutamine and 1% penicillin/streptomycin) at 5×10^5 cells/ml. One hundred microlitres of cells were added to microtitre wells containing 0.5 or 1.0 μl of an appropriately diluted compound solution. After the assay plates had been incubated for 1 h at 37 °C, 5% CO₂, 25 μl LPS (1 ng/ml final) was added and the samples incubated at 37 °C, 5% CO₂ for a further 20 h. The supernatant was then assayed for TNF-α using a commercially available ELISA (Pharmingen).
- PDE4B2B protein (152–503) was derived from PDE4B2B (152–528) by the action of endogenous protease activity during extraction and purification procedures from insect cells. Purification was performed essentially as described in Rocque et al. (Protein Expr. Purif. **1997**, *9*, 191) but with some modifications. During cell breakage and extraction of Sf9 insect cells expressing human PDE4B2B (152–528) protease inhibitors were not included to promote cleavage. After clarification by centrifugation and filtration PDE4B2

protein was purified on Q-Sepharose FF and Cibacron Blue Sepharose FF as previously described. The eluate was applied to a 10 ml Q-Sepharose HP column and eluted with a NaCl gradient to separate cleaved from uncleaved protein. The cleaved protein was further purified by size exclusion on a Superdex 200 column (26 × 60) and finally dialysed into 10 mM Hepes, pH 7.0, 20 mM NaCl, 0.1 mM EDTA for crystallography. The site of cleavage was confirmed by LC-MS/MS on the C-terminal peptide from a trypsin digest using an LCQ Deca XP Plus ion trap mass spectrophotometer. Purified protein was concentrated to 16–20 mg/ml in 10 mM Hepes, pH 7.0, 20 mM NaCl, 0.1 mM EDTA. Diffraction quality crystals were obtained using a modified condition to that described by Xu, et al. (*Science* **2000**, 288, 1822). The crystals were grown at 4 °C by vapour diffusion using an equal volume of protein to well solution (14–18% PEG 3000, 10% glycerol, 50 mM sodium cacodylate, pH 6.5, 100 mM sodium acetate, 1 M sodium chloride, 1% DMF and 5 mM DTT). Crystals typically grew up to 0.5 mm in length within 1–4 weeks. The complex

structure was obtained from a crystal soaked with 1 mM inhibitor (compound **20a**) for approximately 3 days in well solution containing 18% PEG 3000. X-ray diffraction data were collected at 100 K at wavelength 0.933 Å using beamline ID14.4 with an ADSC Quantum 4 CCD detector at the European Synchrotron Radiation Facility. The data were processed with HKL data processing package (Otwinowski, Z., Minor, W. *Methods Enzymol.* **1997**, 276: *Macromolecular Crystallography*, part A, p. 307) and the structure solved using molecular replacement starting from the native pde4b coordinates (molecule A of PDB entry 1f0j) as the search model in Amore (Navaza *J. Acta Cryst.* **1994**, A50, 157) followed by refinement by REFMAC (Murshudov, et al. *J. Acta Cryst.* **1997**, D53, 240). Three surface cysteines in the crystal structure have been modelled with an associated Arsenic atom as they appear to be chemically modified (at least partially) possibly due to cacodylate in the crystallisation buffer (Maignan et al. *JMB* **1998**, 282, 359). The final R-factor achieved for the complex was 19.9% (R-free = 24.1%) and the coordinates deposited in the PDB as entry 3D3P.